Journal of Materials Research and Technology 44 (2026) 3386–3397

Contents lists available at ScienceDirect

Journal of Materials Research and Technology

journal homepage: www.elsevier.com/locate/jmrt

Comprehensive study of mechanical, structural, magnetic, and biological properties of magnetic PLA composites for 3D and 4D printing applications

Kinga Kardos [a], Emese Paari-Molnar [a,*], Roland Told [a], Wa'el Nafith Abdel-Fattah Qa'dan [a,b,c], Peter Szabo [d,e], Alexandra Steinerbrunner-Nagy [f], Adam Tibor Schlegl [b], Judit E. Pongracz [f], Peter Maroti [a]

[a] 3D Printing and Visualization Centre, Medical School, University of Pecs, 2 Boszorkany Rd., Pecs, H-7624, Hungary
[b] Department of Orthopaedics, Medical School, University of Pecs, Akac Str. 1, Pecs, H-7632, Hungary
[c] Department of Prosthetics and Orthotics, School of Rehabilitation Sciences, University of Jordan, Al Qabas, Amman, Jordan
[d] Department of Biophysics, Medical School, University of Pecs, 12 Szigeti St., Pecs, H-7624, Hungary
[e] Environmental Analytical and Geoanalytical Research Group, Szentagothai Research Centre, University of Pecs, 20 Ifjusag str., Pecs, H-7624, Hungary
[f] Department of Pharmaceutical Biotechnology, Faculty of Pharmacy, University of Pecs, Rokus Str. 2, Pecs, H-7624, Hungary

A R T I C L E I N F O

Keywords:
3D printing
PLA
Magnetic
Composites

A B S T R A C T

Metal composites containing magnetic metals are popular materials for 3D printing using Fused Filament Fabrication (FFF) technology. The present study investigates the mechanical, structural, thermal, biological, and magnetic properties of three commercially available magnetic polylactic acid (PLA) composites and pure PLA 3D printed with FFF technology. In this research, a comprehensive array of mechanical testing methodologies was performed including tensile, flexural, Charpy impact and Shore D hardness tests. In addition, scanning electron microscopy imaging, electric resistance, magnetic deflection measurements and thermal conductivity measurements were conducted. Cytotoxicity was measured using the A549 cell viability assay. The results of the mechanical tests showed that the lowest flexural properties were measured in the case of ColorFabb SteelFill (flexural strength: 34.1 MPa ± 0.68 MPa and strain at maximal flexural stress: 1.46% ± 0.06%). It also had the lowest tensile modulus (19.2 MPa ± 0.24 MPa). None of the composites investigated had a cytotoxic effect in short-term contact, and interestingly none of them was electrically conductive. Furthermore, two of the composites (ColorFabb SteelFill and ProtoPasta Iron-filled) have deflected under the influence of homogenous magnetic field. These findings suggest that the examined materials have potential for external biomedical application, along with the possibility of their use in 4D printing.

1. Introduction

Additive manufacturing (AM) is a group of technologies used to create physical objects by adding material as specified by a 3D model. The most commercially available AM process is material extrusion (MEX), particularly Fused Filament Fabrication (FFF) [1,2]. Although initially developed as a rapid prototyping process, FFF has since evolved into a revolutionary manufacturing technology with a broad spectrum of applications ranging from hobbyist activities to industrial production [3].

The use of AM technologies has emerged an innovative advancement in biomedical engineering and healthcare [4]. Numerous studies confirm the usefulness of AM in medical education, preoperative surgical planning, the development of medical devices and the fabrication of orthoses, prostheses and implants with high anatomical accuracy [5–14].

The most frequent materials utilized for FFF are thermoplastic polymers, but there has been a recent surge in the use of additives such as wood, ceramic, carbon or metal particles [15–18]. The increasing interest among consumers in aesthetically appealing 3D-printed objects, combined with the escalating level of research attention has led to a rise in the popularity of metal-filled printing materials [15]. The addition of metal particles into a polymer matrix can improve various material properties, including tribological, mechanical and thermal behavior, as well as electrical and magnetic properties [19].

In addition, the integration of various types of metal fillers into

* Corresponding author.
E-mail address: paari.molnar.emese@pte.hu (E. Paari-Molnar).

https://doi.org/10.1016/j.jmrt.2026.07.320
Received 27 May 2026; Received in revised form 20 July 2026; Accepted 31 July 2026
Available online 16 August 2026

polymer matrix materials has the potential to expand the applications of these materials in the biomedical field through 4D printing [20,21]. The concept of 4D printing represents an evolution of the 3D printing paradigm by introducing the fourth dimension of time. The technology utilizes smart materials, including smart polymers, shape-memory materials and hydrogels, which exhibit programmable responses to specific environmental stimuli, resulting in alterations to their structural or geometrical characteristics [22].

A particularly promising external stimulus for metal containing polymers is stimulation by an electromagnetic field. Certain metal-polymer composites exhibit magnetic properties due to the presence of magneto-responsive particles, such as iron or iron-based alloys (stainless steel, maraging steel). These fillers are among the most researched due to their favorable magnetic characteristics and good thermal and mechanical properties. Therefore, they are used in both custom-developed and commercially available materials [23–26].

A study by Bernier et al. investigated 3D-printed composites containing different hard and soft magnetic materials in polyamide matrix material. It was observed that the addition of a greater amount of magnetic powder to the composite resulted in a corresponding increase in the stiffness of the material. Due to the weak fusion between the layers, the 3D printed samples were of bad quality [27].

In a previous article, different amounts of carbonyl iron powder were added to PLA to fabricate a magnetic filament for FFF technology. It has been demonstrated that saturation magnetization and remanence are directly proportional to the amount of the filler. The average tensile strength of the composites was slightly higher than that of the pure PLA [28].

In a study by Díaz-Gracia et al., PLA-based composite with 30 wt%, 39 wt% and 52 wt% of gas-atomized magnetic maraging steel was developed for 3D printing and characterized by mechanical, thermal, rheological and magnetization measurements. The composite showed soft magnetic character [29]. Cao et al. fabricated magneto-active actuators using a self-developed flexible magnetic filament utilizing thermoplastic rubber and carbonyl iron particles and found that the printing orientation, thickness and length of the sample all affect the deflection under the magnetic field. Specifically, 0°orientation, a thinner or a longer beam appears to be more sensitive to deformation [30].

A few studies have already been conducted on the 3D printing of polymers containing magnetic particles in the biomedical field. Zhao et al. designed a 3D printed bone tissue scaffold from a custom-developed shape memory PLA/Fe_3O_4 composite, using a magnetic field as an actuation mechanism to change the shape of the device. The shape recovery ratio was higher than 95.5% suggesting that it may potentially be a suitable technique for making a minimally invasive implant [31].

A group of commercially available PLA/magnetic metal composites was selected for investigation, representing a subset of available materials in this category. In a study by Hasanzadeh et al., the printing parameters of a PLA composite containing iron particles (Iron-filled by ProtoPasta) were investigated [14]. To find the optimal parameters (nozzle temperature, printing speed and nominal porosity) the authors have used the Response Surface Methodology technique. The study has found that the greatest effect for the Charpy impact strength has the nominal porosity, while the least effect has the nozzle temperature for it. Another study investigated the properties of ProtoPasta Iron-filled composite material also [32]. The authors found that the stiffness of this Iron-filled PLA composite was significantly lower than that of pure PLA, but the tensile strength of the composite was suitable. Dezaki et al. investigated the possibility for sustainability of ProtoPasta Iron-filled composite with ProtoPasta Conductive PLA [26]. It was found that these composites may be suitable for 4D printing using electric current as an external stimulus.

A study by Pan and coworkers investigated the tensile properties of ProtoPasta Iron-filled and Steel-filled (filled with stainless steel particles) [33]. The study found that all tensile properties of the composites were reduced compared to the pure PLA.

Tedla and coworkers studied another PLA composite with magnetic filler, ColorFabb SteelFill material, which contains stainless steel powder [15]. It was found that the metal particles can be easily removed from the filament and the 3D-printed objects. Alnajjar et al. investigated possible designs for NMR magnets using ColorFabb Steelfill material [34]. These magnets can be used in MRI machines.

Metal filled polymer composites combine the ease of processing characteristics of polymers with the magnetic and mechanical properties of metals; therefore, their thorough investigation is both necessary and highly warranted. Interestingly, the mechanical properties of these composites have not yet been comprehensively examined in previous studies, but only individual properties have been investigated. This facilitates the fabrication of distinctive structures that can be regulated by an external magnetic field, a capability that is of particular value in the domain of medical technology, for instance in the development of shape-memory implants, soft robots, or targeted drug delivery systems. In this context, the aim of the present research is to investigate the comprehensive material technology and magnetic properties of commercially available polymer-metal composites and to explore the extent to which these composites are suitable for 4D printing and medical use. Mechanical (tensile, flexural, Charpy impact, and Shore D hardness) tests, thermal conduction measurements, magnetic deflection measurements, and electrical resistance measurements were performed. Cell viability tests were also carried out. A further objective of the research is to formulate specific biomedical application suggestions based on the results.

2. Materials and methods

In this study, PLA-metal composites with magnetic properties that do not require a sintering process have been investigated. The total number of specimens is 74. Fig. 1 represents the protocol of the study.

2.1. Test materials and specimen preparation

The specimens for the examinations were produced by FFF technology, using a Craftbot + tabletop 3D printer (Craftbot Ltd., Salgótarjáni rd. 12–14., Budapest 1087, Hungary). The utilized materials were the following: pure PLA (Herz Hungária Kft., Pesti rd. 284., Üllő 2225, Hungary), SteelFill (ColorFabb, Bremweg 7, 5951 DK Belfeld, The Netherlands) and Steel-Filled Metal Composite PLA (Protopasta, Protoplant Inc, 12001 NE 60th Way, Suite B-2, Vancouver, WA 98682, US), which are PLA filaments with a high amount of stainless steel particles; and Iron-Filled Metal composite PLA (Protopasta, Protoplant Inc, 12001 NE 60th Way, Suite B-2, Vancouver, WA 98682, US), a ferromagnetic filament with iron powder [35,36]. All materials are commercially available. The filament diameter was 1.75 mm for all materials. For all investigated materials the printing parameters were identical: the nozzle diameter was 600 μm, the extruder temperature was 210 °C, the heated bed temperature was 50 °C, and the specimens were printed in 'XY' orientation with 200 μm layer height and 100% infill, the printing speed was set to 30 mm/s, the raster angles were 45°and −45°. These printing parameters were chosen during the printing optimization process.

2.2. Mechanical tests

All mechanical tests were performed five times in accordance with the relevant standard, and all samples were conditioned at 23 °C ± 1 °C for at least 4 h in accordance with ISO 291:2008 [37].

2.2.1. Tensile test

To evaluate the tensile characteristics of printed polymer-metal composites, tensile tests were conducted using a Zwick/Roell Z100 THW universal material tester (ZwickRoell, 89079, August-Nagel-Straße

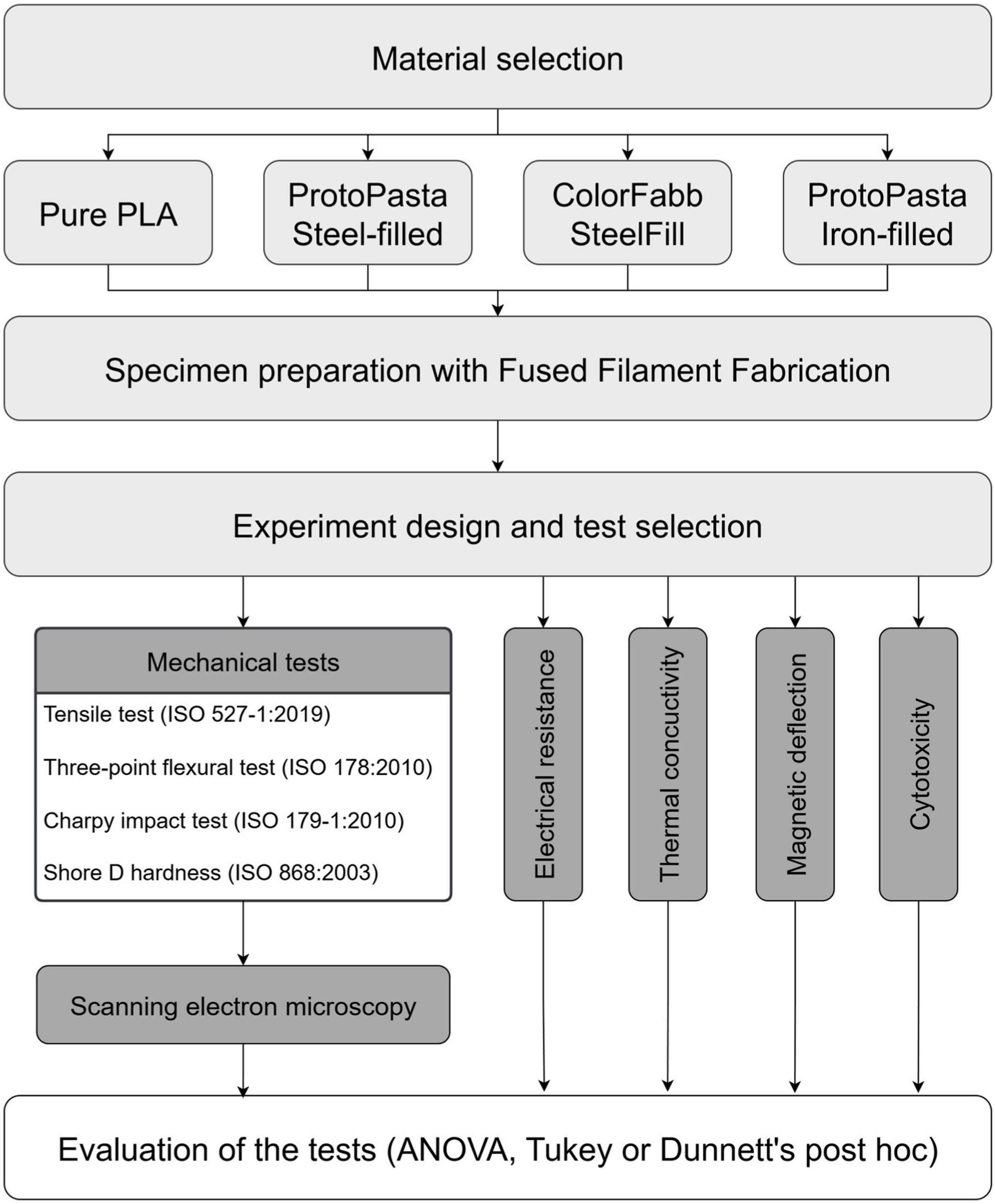

Fig. 1. Experimental protocol.

11 Ulm, Germany) with an extensometer. The measurements were performed in accordance with ISO 527-1:2019 standard for polymer-metal composites with A5 specimens (ISO 527-2:2012) [38]. For the measurements, the preload was set to 0.1 MPa and the test speed was 1 mm/min for Young's modulus determination and 2 mm/min for the rest of the test.

2.2.2. Three-point flexural test

The three-point flexural tests were conducted using the same Zwick/Roell Z100 THW universal material tester. The tests were carried out according to ISO 178:2010 standard using preferred test specimens (80 mm × 10 mm x 4 mm) [39]. The preload was 0.1 MPa and the test speed was set to 2 mm/min throughout the test.

2.2.3. Charpy impact

The impact values of the specimens were measured by a Zwick/Roell HIT50P (ZwickRoell, 89079, August-Nagel-Straße 11 Ulm, Germany) instrument utilizing a 5 J pendulum. The tests were performed based on ISO 179-1:2010 standard [40], using Type 1 test specimens with dimensions of 80 mm × 10 mm x 4 mm.

2.2.4. Shore D hardness

A Zwick/Roell 3131/320154 (ZwickRoell, 89079, August-Nagel-Straße 11 Ulm, Germany) instrument was utilized for the Shore D hardness tests, which was on a stable stand during the entire measuring period. The tests were performed in accordance with the ISO 868:2003 standard [41].

2.3. Mass ratio calculations

For all investigated metal-filled composites, the proportion of the filler material was estimated. The method to estimate the mass and volume ratio is the same as in a previous study [21]. A Steinberg Systems SBS-LW-300A precision balance (Steinberg Systems expondo GmbH, 10963, Dessauer 28-29 Straβe, Berlin, Germany) was used to measure the mass of a 100 mm filament of each composite. The density of the filament can be calculated in the following steps:

$$\rho_{\text{filament}} = \frac{m}{l \cdot d^2 \frac{\pi}{4}}, \tag{2}$$

where ρ_{filament} is the density of the filament in g/cm^3, m is the measured mass of the filament in g, l is the length of the filament in cm, and d is the diameter of the filament in cm. The mass ratio of the composite can be calculated:

$$\frac{m_{\text{metal}}}{m} = 1 - \frac{\rho_{\text{PLA}}}{\rho} \cdot \frac{\rho - \rho_{\text{metal}}}{\rho_{\text{PLA}} - \rho_{\text{metal}}}, \tag{3}$$

where m_{metal} is the mass of the metal part of the filament in g, m is the mass of the filament in g, ρ_{PLA} is the density of PLA in g/cm^3, ρ is the density of the filament in g/cm^3, ρ_{metal} is the density of the filler in g/cm^3.

2.4. Scanning electron microscopy

Scanning electron microscopy analyses were conducted on both the intact surface and fracture surface of the Charpy specimens to examine the material's microstructure. The imaging was carried out with JEOL JSM-IT500HR device (3–1–2 Musashino, Akishima, Tokyo 196–8558, Japan) using 50x and 250x magnification. Additionally, providing further insight into the composition of the materials, elemental analysis was performed using the energy-dispersive X-ray spectroscopy (EDS) method with a silicon drift detector (SDD).

2.5. Electrical resistance tests

Electrical resistance tests were carried out using a Rohde & Schwarz HMC 8012 Digital Multimeter (Rohde & Schwarz GmbH & Co KG, Munich, Germany). The specimen size was 100 mm × 5 mm x 1.2 mm. The tests were carried out on 5 specimens, three times for all investigated materials.

2.6. Thermal conductivity

The thermal conductivity factor of the investigated materials was determined in the same way as in a previous publication [21]. The shape of the specimens is a disk with a diameter of 35 mm, and a thickness of 5 mm. Fig. 2 represents the scheme of the measurement. The thermal conductivity factor was determined at 33 °C, 37 °C and 40 °C temperatures.

The measurement was controlled by an Arduino UNO (Arduino, Sommerville, MA, US). Temperature was measured by two NTC temperature sensors (100 kΩ resistance) on the opposite circular surfaces of the disk specimens. Heating was provided by a Rohde & Schwarz NGE100 Power Supply Series (Rohde & Schwarz GmbH & Co KG, Munich, Germany), which was controlled by a F ~ TEK SSR-10 DD Solid State Module (Techfun s. r. o., Žaškov, Slovak Republic). The power [W] was measured with a Rohde & Schwarz HMC 8012 Digital Multimeter (Rohde & Schwarz GmbH & Co KG, Munich, Germany). The heat flow ($\dot{Q}$ [W]) can be calculated by deducting the heat loss from the measured power. The thermal conductivity was calculated by the following equation [42]:

$$\lambda = \left| \frac{\dot{Q}}{A \cdot \frac{T_2 - T_1}{\delta}} \right|, \tag{1}$$

where λ [W/(mK)] is the thermal conductivity factor, $\dot{Q}$ [W] is the heat flow, A [m^2] is the cross section of the specimen, δ [m] is the distance between the two measurement points, T_1, T_2 [K] are the measured temperatures at the surfaces of the specimen.

Thermal conductivity was measured on three specimens three times for all the investigated materials.

The thermal conductivity coefficients for pure PLA material have not been determined. Consequently, the present study utilized data that had been measured in a preceding study [21].

2.7. Magnetic deflection

One of the most frequently studied magnetic properties is magnetic deflection. The effect of the magnetic field on the magnetizable material is examined. The experiment was designed based on the article [30]. A neodymium magnet was used to create a homogeneous magnetic field. Magnetic induction was measured with a PCE-MFM- 4000 Electromagnetic Field Meter (PCE Deutschland GmbH, Im Langel 4, 59872

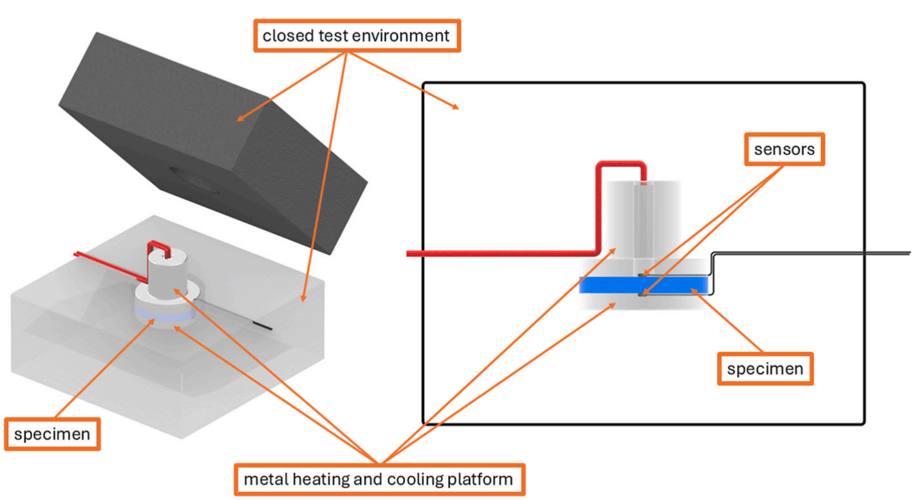

Fig. 2. Schematic representation of the thermal conductivity test [21].

Meschede, Germany). Magnetic deflection was measured at various distances between the specimen and the magnets. For the Colorfabb Steelfill material, the range is 75 mT to 95 mT, whereas for ProtoPasta materials, it is 75 mT to 120 mT. Fig. 3 shows the experimental scheme of measurement. The size of the specimens is 100 mm × 5 mm x 1.2 mm, the same as in the electrical resistance measurements. The magnetic deflection measurements were carried out on five specimens, three times for all investigated composites. The deflection was determined using a photograph and the JMicroVision software [43]. Millimeter paper, as shown in the measurement setup (Fig. 3.), was used to calibrate the software.

2.8. *Cytotoxicity measurements*

2.8.1. *Cell culturing and treatment*

A549 cells (ATCC, 10801 University Blvd Manassas, VA 20110, US, Cat. no: CRM-CCL-185) were maintained in DMEM (Dulbecco's Modified Eagle's Medium – Lonza Group AG, Muenchensteinerstrasse 38, 4002 Basel, Switzerland, Cat. no: 12604F), supplemented with 10% FBS (Fetal Bovine Serum – Euroclone S. p.A, Via Figino 20/22, 20016 Pero (MI), Italy, Cat. no.: ECS0180L), 100 U/ml of penicillin–streptomycin (Lonza Group AG, Muenchensteinerstrasse 38, 4002 Basel, Switzerland, Cat. no.: DE-17-602E), 0.1 mM non-essential amino acids (Lonza Group AG, Muenchensteinerstrasse 38, 4002 Basel, Switzerland, Cat. no: 13-114E), 10 mM Hepes (Lonza Group AG, Muenchensteinerstrasse 38, 4002 Basel, Switzerland, Cat. no: 17-737E) and diluted β-mercaptoethanol (Thermo Fisher Scientific's, 168 Third Avenue, Waltham, MA 02451, US, Cat. no: 21985–023). The cells were cultured at 37 °C under 5% CO2 in humidified atmosphere.

A549 cells were resuspended in 1 ml of DMEM media, seeded at a density of $3x10^4$ cells/well on the surface of a 24-well plate, and then incubated for 8 h at 37 °C in humidified environment with 5% CO2.

Following the attachment of the cells to the cell culture plate's surface, the printed synthetic inserts composed of different materials were inserted into each well and cultured for 48 h. The inserts' surfaces were exposed to UV light twice for 30 min each time they were inverted to avoid contaminating the cell cultures.

To determine the total nucleic acid content, propidium iodide (PI) (Sigma-Aldrich, Cat. No.: 81845) staining was used. A549 cells treated with 1 μM Staurosporine (Sigma Aldrich, 3300 S2nd St., St. Louis, MO 63118, US, Cat. no: S-6942) served as positive controls for detecting apoptotic cell death. For each material group, three independent printed inserts were tested in each experimental run (n = 3 per run). The complete cytotoxicity experiment was repeated three independent times using newly prepared inserts in each experiment. Therefore, a total of nine independent inserts were evaluated per material group (n = 9).

2.8.2. *Living cell number quantification based on total nucleic acid content determination*

The detected fluorescence intensity of propidium iodide (PI) staining (Sigma-Aldrich, 3300 S2nd St., St. Louis, MO 63118, US, Cat. no: 81845) served as the basis for the applied cell viability experiment. The method differed from the conventional PI staining procedures. The total nucleic acid content was determined using PI staining on the PerkinElmer EnSight Multimode plate reader (PerkinElmer, 710 Bridgeport Ave, Shelton, CT 06484, US) following a 48-h exposure to the synthetic inserts. In summary, the treated cells were rinsed in 500 μl of PBS (phosphate buffered saline) (pH 7.4) to eliminate the detached apoptotic cells. Adherent, live cells were lysed in 500 μl of cell-lysing borate solution (pH 9.2) after apoptotic cells were removed, and PI was added at a concentration of 2 μg/ml.

Following a 5-min incubation period in a dark environment on an orbital shaker, fluorescence intensity was measured at wavelengths of $\lambda_{emission} = 620$ nm and $\lambda_{excitation} = 530$ nm. The results of every treated sample were compared to the untreated controls.

2.9. *Statistics*

The measured mechanical results obtained were examined using Origin Pro software (OriginLab Corporation, One Roundhouse Plaza, Suite 303, Northampton, MA 01060, USA). The results were analyzed using the Shapiro-Wilk normality test, and a one-way ANOVA test was performed with a Tukey post hoc test; the confidence interval was set at 95%. The validity of the statistics was verified using power analysis. For all statistical probes the sample size was 5 for the mechanical properties. All statistical results of the mechanical test can be found in the supplementary material.

Statistical analyses of the cytotoxicity test were performed using GraphPad Prism version 8. Data distribution was assessed using the Kolmogorov–Smirnov normality test normality (significant levels were labeled as follows: $p < 0.0332$ (*), $p < 0.0021$ (**), $p < 0.0002$ (***), and $p < 0.0001$ (****)., and variance homogeneity was evaluated before

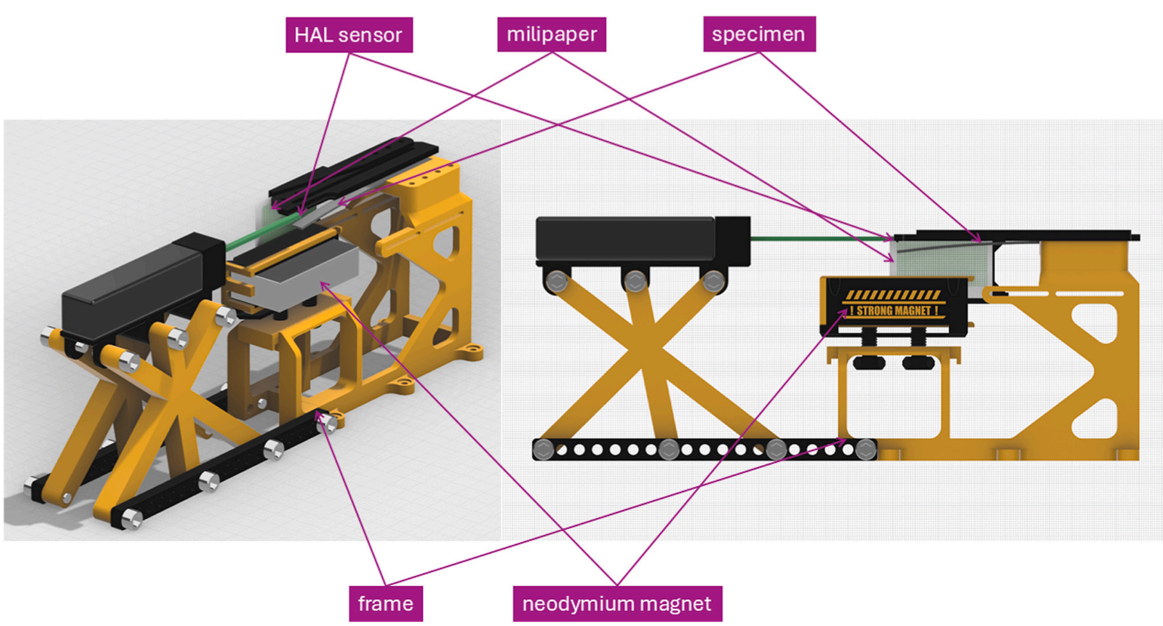

Fig. 3. Experimental scheme to measure magnetic deflection.

applying parametric tests. Since each material group was compared with the untreated control group, one-way ANOVA followed by Dunnett's multiple comparisons test was applied. Statistical significance was defined as $p < 0.05$.

3. Results

3.1. Mechanical test

3.1.1. Tensile and three-point flexural test

For each material, five tensile specimens were tested until failure, and their tensile Young's modulus, tensile strength and elongation at tensile strength were detected. As seen in Fig. 4, the highest tensile Young's modulus was observed for the PP Steel-filled with a value of 4735 MPa ± 39.1 MPa, which was significantly higher than that of other materials. Another composite from this manufacturer, the PP Iron-filled had a similar modulus, 4539 MPa ± 53.8 MPa, but based on the statistical probe, it also differed significantly. Interestingly, the lowest Young's modulus was observed for the other stainless steel-containing composite, the CF SteelFill, with 3005 MPa ± 30.2 MPa, which was lower than pure PLA.

The tensile strength and elongation at tensile strength of the pure PLA were found to be 54.1 MPa ± 1.73 MPa and 1.98% ± 0.03% (Fig. 5 a)), respectively, representing the highest values measured. It is noteworthy that the lowest tensile strength measured for the CF Steel, 19.2 MPa ± 0.24 MPa, constituted only a little over a third of the highest tensile strength observed.

During the three-point flexural test, only the pure PLA did not break until the end of the measurement period, and its stress at conventional deflection was 86.2 MPa ± 3.88 MPa (Fig. 5 b)). Similar to the tensile Young's modulus, the flexural Young's modulus of the PP Steel-filled was the highest, 4154 MPa ± 46.6 MPa. Nevertheless, it did not differ significantly from PP Iron-filled (4031 MPa ± 70.6 MPa). The highest flexural strength and strain at maximal flexural stress were observed for the PP Iron-filled, with a value of 75.5 MPa ± 1.12 MPa and 2.97% ± 0.03%. Of the four materials investigated, the pure PLA was the most flexible in the flexural test, with a Young's modulus of 2703 MPa ± 122 MPa, and the lowest flexural strength (34.1 MPa ± 0.68 MPa) and strain at maximal flexural stress (1.46% ± 0.06%) were measured for the CF SteelFill material.

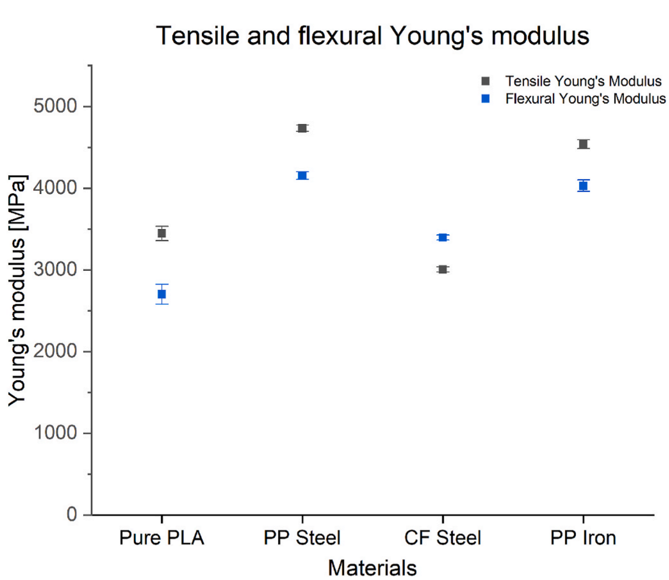

Fig. 4. Tensile and flexural Young's modulus of magnetic PLA-metal composites.

3.1.2. Charpy impact test and shore D hardness

The Charpy impact strength exhibited a range between 9.98 kJ/m^2 ± 0.26 kJ/m^2 (CF SteelFill) and 17.0 kJ/m^2 ± 0.12 kJ/m^2 (PP Iron-filled), demonstrating a significant difference across all cases (Fig. 6).

The Shore D hardness of the PP Steel-filled was the highest, with the value of 76.3 ± 1.34, but the hardness of the PP Iron-filled and the pure PLA did not differ significantly, as illustrated in Fig. 6. The lowest value was measured for CF SteelFill, which was 68.9 ± 2.89.

3.2. Mass ratio calculations

The density of each material was determined and compared with the manufacturer's data. The metal content of the composite materials was also determined. The collected data (ρ: density (g/cm^3), m_{metal}/m: mass ratio (%)) are represented in Table 1.

3.3. Electrical resistance tests

None of the materials investigated conducted electrically.

3.4. Scanning electron microscopy

Fracture surfaces of the Charpy specimens were examined by scanning electron microscopy to investigate the internal structure of the composites. The original SEM pictures of the composites can be found in the Supplementary materials, located in the SEM folder.

SEM images of pure PLA at 50× magnification revealed the presence of pronounced interlayer and intralayer porosity, appearing as longitudinal gaps and large voids, indicating that the layer fusion was not fully completed during the printing process (Fig. 7 a)). The interlayer porosity can also be observed in PP Steel-filled and PP Iron-filled materials though to a lesser extent (Fig. 7 b) and d)). In the case of PP Steel-filled, it appears as thin lines between layers, while in the case of the PP Iron-filled composite, it is characterized by the presence of triangular-shaped pores. For the CF SteelFill the layer adhesion was almost defined, with only a limited number of small pores being visible (Fig. 7 c)).

The presence of metal particles in the products of the two manufacturers is observed in a variety of forms (Fig. 8). The metal fillers utilized in Protopasta products exhibited irregular shapes and are coated with the matrix material. Furthermore, aggregates can be observed in certain areas, primarily for the PP Iron-filled material. The size of the metal particles was between 5 μm and 25 μm for the PP Steel-filled composite, whereas the size of the filler aggregates was between 10 μm and 45 μm for the PP Iron-filled material. In contrast, the metal particles in CF SteelFill are clearly visible and present in substantial numbers. The steel particles exhibited spherical shape, and their distribution is more homogeneous. The diameter of the metal spheres demonstrates a variability range from 5 μm to 20 μm.

3.5. Thermal conductivity

The thermal conductivity factor was determined for each material investigated (Fig. 9). The standard deviation of the results of the metal-filled composites is similar in magnitude, in the case of pure PLA, this value is significantly lower. Pure PLA has the lowest thermal conductivity factor: 0.038 W/(mK) ± 0.018 W/(mK) at 37 °C. The thermal conductivity factor of the two PP materials is in the same range: PP Steel-filled: 0.127 W/(mK) ± 0.051 W/(mK), PP Iron-filled: 0.127 W/(mK) ± 0.051 W/(mK) at 37 °C, the CF SteelFill has higher thermal conductivity factor: 0.343 W/(mK) ± 0.048 W/(mK) at 37 °C.

3.6. Magnetic measurements

Magnetic deflection measurements were carried out for all examined magnetic materials. Five specimens were measured three times for all the composites investigated.

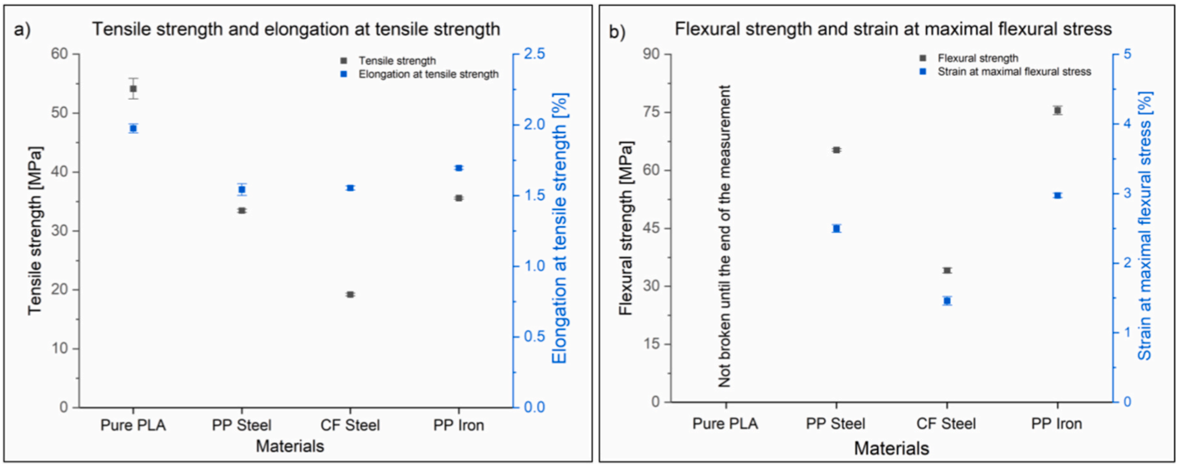

Fig. 5. Tensile and flexural properties of magnetic PLA-metal composites. a) Tensile strength and elongation at tensile strength, b) Flexural stress and strain at the maximal flexural stress of the materials.

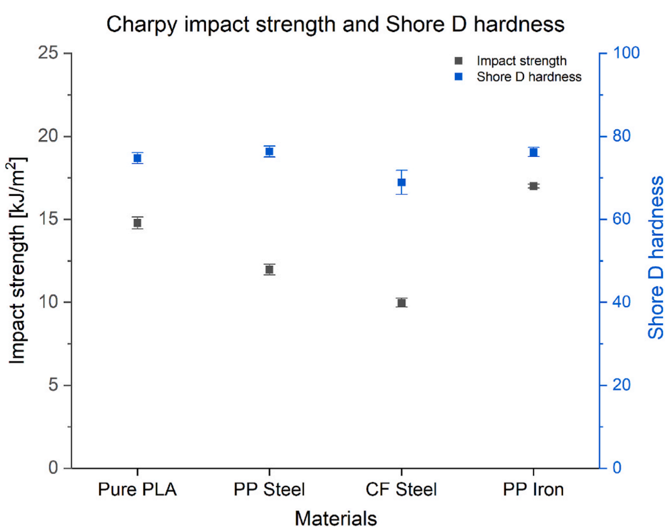

Fig. 6. Results of the Charpy and Shore D hardness test of the magnetic PLA-metal composites. Black squares indicate the Charpy impact strength with the standard deviation, and blue squares show the Shore D hardness of the materials with standard deviations.

Table 1
Density and metal content of the investigated materials. Comparing the manufacturer's data with the calculated data. Abbreviations: PP: ProtoPasta, CF: ColorFabb.

Material	Manufacturer's data		Calculated data		Deviation from manufacturer's data	
	ρ (g/cm^3)	m_{metal}/m (%)	ρ (g/cm^3)	m_{metal}/m (%)	$\Delta(m/m)$ (%)	$\Delta(\rho)$ (%)
Pure PLA	1.24	0	1.22	0	N/A	1.30
PP Steel-filled	2.3	60	2.22	52.3	12.79	3.65
CF SteelFill	3.13	80	3.24	71.7	10.36	3.65
PP Iron-filled	1.85	45	1.89	40.9	9.11	2.25

The PP Steel-filled material showed no magnetic properties during magnetic deflection tests, but it did react very weakly to magnetic fields. For the CF SteelFill material, the magnetic deflection was higher than that of the PP Iron-filled composite. Fig. 10 represents magnetic deflection depending on the magnetic induction for CF SteelFill and PP Iron-filled materials for the investigated 5-5 specimens.

Based on the results of the magnetic measurement, further investigation was conducted to assess the potential applications of these composite materials' magnetic properties in 4D printing. Although two of the tested composites exhibited magnetic behavior, the high stiffness of the PLA matrix has made it challenging to achieve optimal functionality through elastic deformation of the material. Therefore, a structure has been designed to facilitate gripping through a hinge-like joint, rather than material deformation. In the constructed model, when a magnet is brought into proximity, the resulting magnetic field induces the structure to tilt from one configuration to another around a pivot point (Fig. 11 a)-b)). This motion reduces the cross-sectional shape of the structure, allowing it to be inserted into a hollow cylinder (Fig. 11 c)). When the magnet moved further away (in a higher position), the structure tilted back to its original state, thereby securing the cylinder from the inside and allowing to be lifted or relocated (Fig. 11 d)-e)). Following relocation, bringing the magnet closer again causes the structure to tilt again into its compact state, thereby facilitating the removal from the cylinder. A video illustrating the operational mechanics is available in the supplementary materials.

3.7. Cytotoxicity measurements

The cytotoxicity of various metal-filled polymer composites developed for FFF 3D printing was evaluated. Following 48-h standardized in vitro cytotoxicity testing protocols, none of the examined composites exhibited any cytotoxic effects on cultured cells. The fluorescence intensity values obtained from propidium iodide staining exhibited minimal variation, and the cell viability remained consistently high across all samples (Fig. 12), indicating good biocompatibility. In the positive control samples treated with 1 μM Staurosporine, the total nucleic acid content decreased significantly, which confirmed the assay's sensitivity to apoptosis-induced cell death and validated the experimental setup.

4. Discussion

Polymer-metal composites that can be printed using FFF technology are the subject of increasing research, as their material properties can be modified over a wide range by adding various metal additives. Overall, the results demonstrate that these commercially available metal-filled PLA composites cannot be considered a homogeneous material group since their mechanical, morphological, magnetic, and biological properties differ depending on the manufacturer of the filament. These

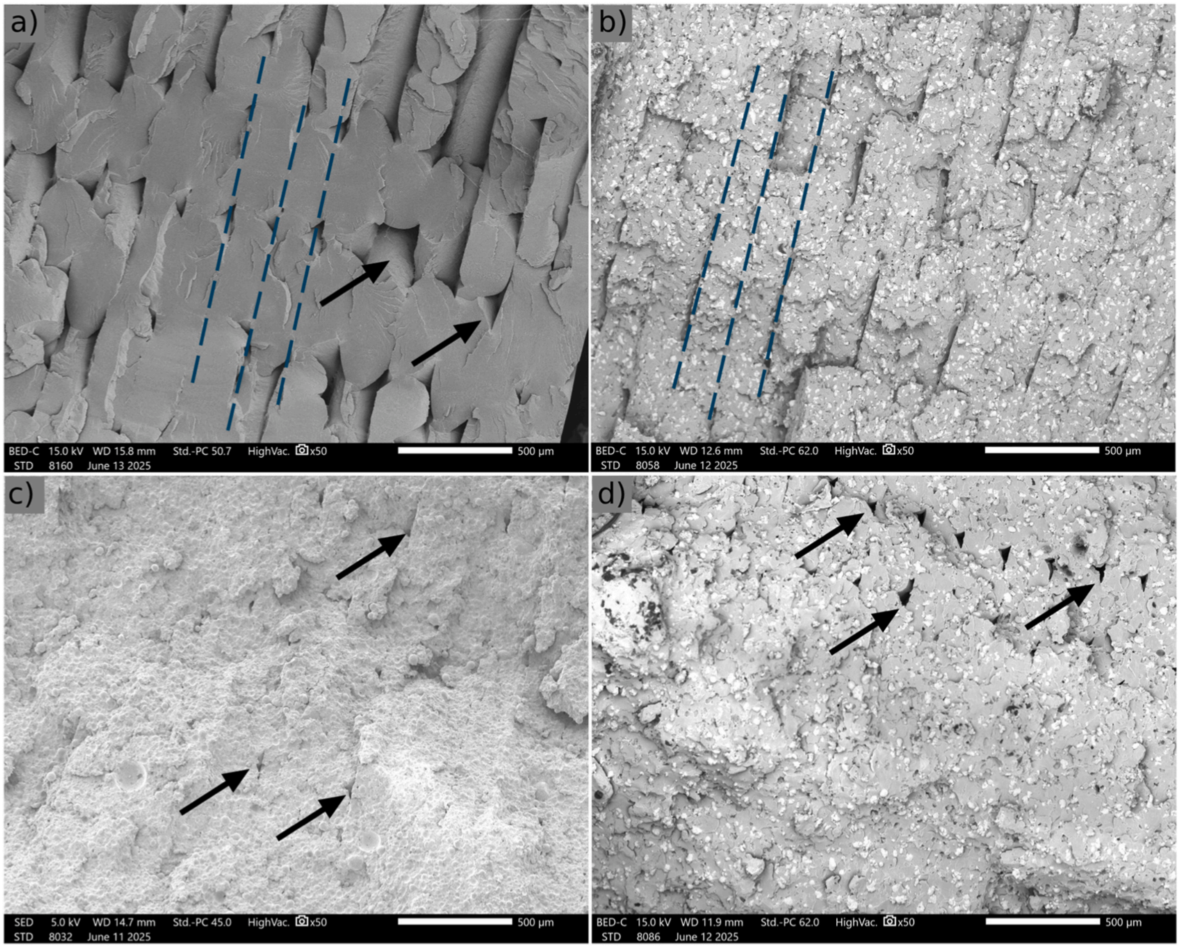

Fig. 7. SEM images of the tested materials at 50x magnification: *a) Pure PLA, b) PP Steel-filled, c) CF SteelFill, d) PP Iron-filled. Arrows indicate gaps between the printing layers; blue dashed lines indicate the layer borders. Abbreviations: PP: Protopasta, CF: ColorFabb.*

differences suggest that the final properties of the 3D-printed specimens are determined not only by the nominal metal content, but also by the particle morphology and distribution within the polymer matrix, and the interaction between the filler and the polymer matrix. The present study focuses on commercially available metal containing PLA composites that are presumed to have magnetic properties. Because of the off-the-shelf type of these materials, the precise composition of them is unknown. To resolve this, we performed a mass-based composition analysis. The measured values differed from those listed in the manufacturer's data sheet by 9% – 13% by weight. Based on the results, the mechanical properties of the examined composites differ significantly from each other and from pure PLA. The tensile strength of pure PLA was higher than that of the metal-filled composites, which can be explained by the presence of metal particles, which can act as stress concentrators within the PLA matrix. Weak adhesion between PLA and metal particles may promote microvoid formation and premature failure. At the same time, the increase in Young's modulus indicates that the metallic filler restricts polymer chain mobility and increases the resistance of the composite to elastic deformation, so the incorporation of metallic particles improves the rigidity while reducing the material's ability to withstand tensile stress before failure. Although the tensile properties of the two ProtoPasta composites were found to be similar, the tensile strength values reported in this study (33.5 MPa $\pm$ 0.27 MPa for PP Steel-filled and 35.6 MPa $\pm$ 0.17 MPa for PP Iron-filled) are lower than those reported by Pan and coworkers, who found the median tensile strength to be 41.139 MPa for the Steel-filled and 49.69 MPa for the Iron-filled composites [33]. However, the aforementioned study reported considerably lower median tensile Young's modulus for these materials (1307.4 MPa for Steel-filled and 1436.3 MPa for Iron-filled), compared to the results obtained in this study. The Young's modulus of Steel-filled was 4735 MPa $\pm$ 39.1 MPa and that of Iron-filled was 4553 MPa $\pm$ 53.8 MPa, which were significantly higher than pure PLA (3448 MPa $\pm$ 86.6 MPa), suggesting that the materials become stiffer due to addition of metals. Tensile properties of the investigated ProtoPasta composites were also determined in another study, where the specimens were printed with varying layer heights than the present work and found that the average tensile Young's modulus was 3910 MPa and 3638 MPa for the Steel-filled and Iron-filled materials [44]. This discrepancy in tensile properties can be attributed to the different printing parameters.

The composite of the other manufacturer, CF SteelFill, also exhibited lower tensile strength than pure PLA, but it was also significantly lower than the other two composites, with a value of 19.2 MPa $\pm$ 0.24 MPa. It is noteworthy that CF SteelFill also exhibited the lowest tensile Young's modulus of all materials examined. These are presumably related to the metal particle content, distribution, and shape. These results suggest that filler-related parameters have a stronger influence than the filler's metallic nature on mechanical performance.

Based on SEM images, the differences in size and shape of the metal particles between the two manufacturers' composites are clearly visible. In both PP composites, the shape of the metal particles was irregular and aggregated in multiple locations. The particle size ranged from 5 μm to 25 μm for the PP Steel-filled, and from 10 μm to 45 μm for the PP Iron-filled composite. These values are roughly consistent with those measured in a study by Laureto et al., where the particle size in Steel-filled material was between 3 μm and 40 μm, and between 3 μm and

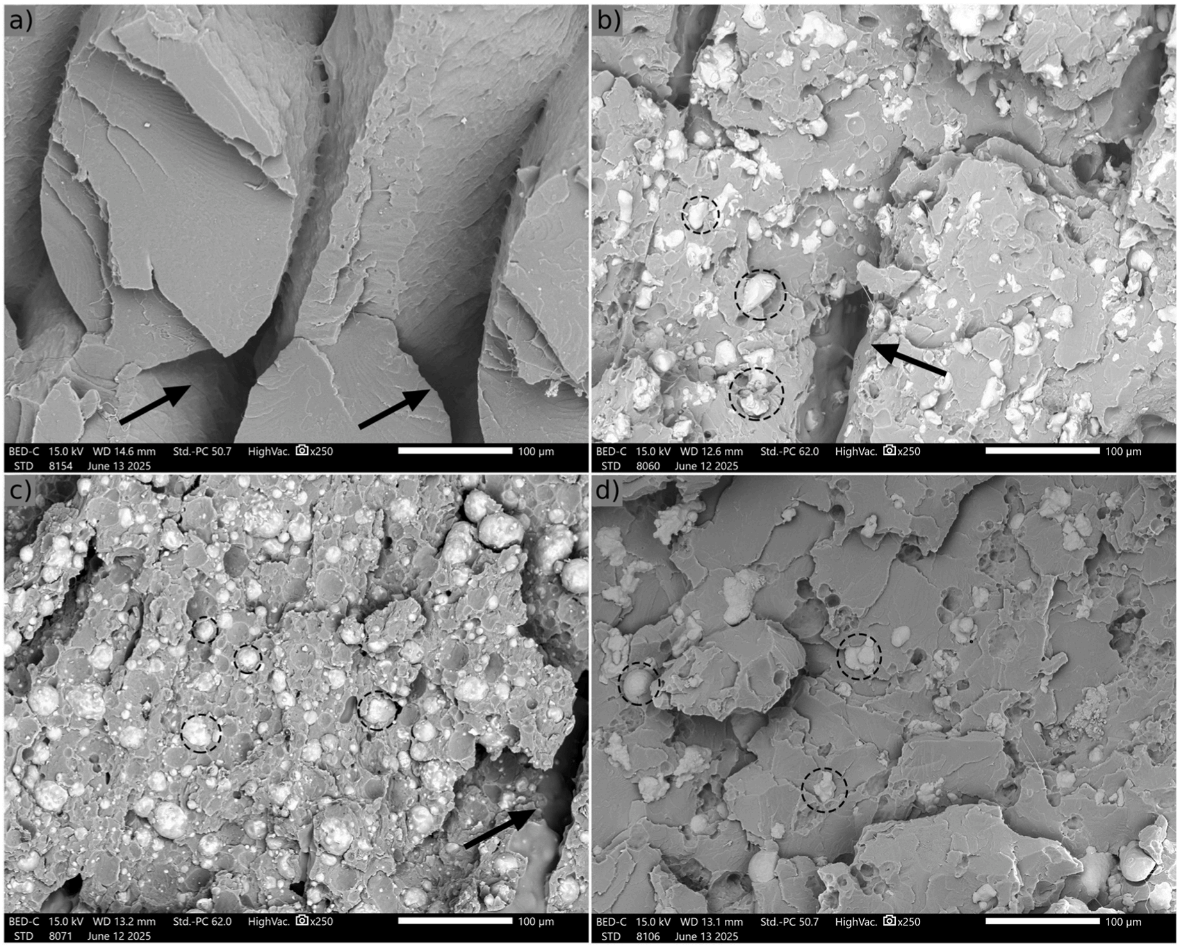

Fig. 8. SEM images of the tested materials at 250x magnification: a) Pure PLA, b) PP Steel-filled, c) CF SteelFill, d) PP Iron-filled. Dashed circles indicate the metal particles or metal aggregates, arrows indicate gaps. Abbreviations: PP: Protopasta, CF: ColorFabb.

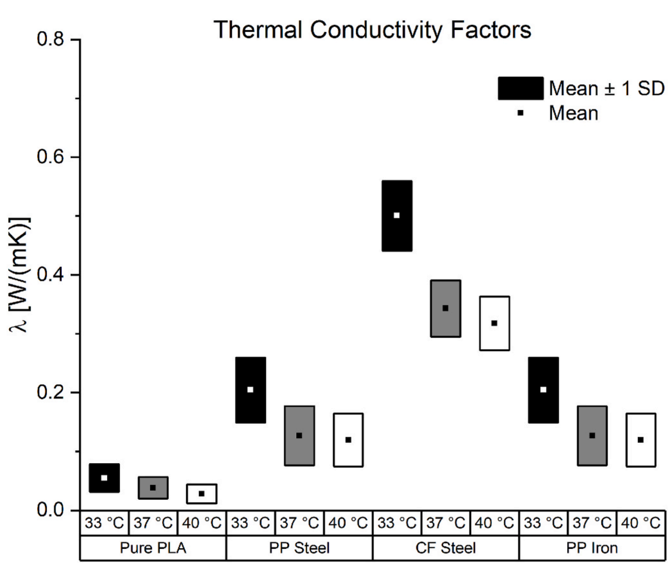

Fig. 9. Thermal conductivity factor for each material investigated. Abbreviations: PP: Protopasta, CF: ColorFabb.

50 μm in Iron-filled material [45]. However, the steel particles in CF SteelFill exhibited spherical morphology, along with a more homogeneous size and spatial distribution. These observations may explain the differences seen in the mechanical tests. Irregular and grouped particles may cause local differences and places where stress builds up, while a more even distribution could mean the material performs better every time. But CF SteelFill, whose particles were rounder and more regular, didn't yield better results, showing that shape alone doesn't explain the results.

The metal-filled materials have also demonstrated different magnetic behavior. Although the CF SteelFill and PP Iron-filled materials exhibited magnetic behavior, the means of the magnetic deflection in the case of CF SteelFill were greater. These differences suggest that the function of these composites is strongly influenced by filler type and distribution. Inhomogeneous distribution may also explain the variation among specimens, as local differences in metal particle concentration can lead to a magnetic response. This hypothesis is further substantiated by the SEM images obtained. In contrast, the PP Steel-filled composite showed very weak magnetic behavior. The magnetic properties of CF SteelFill and PP Iron-filled composite suggest that these materials are potentially suitable for 4D printing, although the stiffness of the matrix material poses a limitation.

The results of the cell viability testing demonstrated that none of the metal-polymer composites exhibited any cytotoxic effect on the A549 cell line in vitro. These findings suggest that incorporating metallic fillers, such as stainless steel or carbonyl iron, into thermoplastics does not inherently compromise the biological safety of the printed material. This is especially promising for biomedical applications, where materials are increasingly required to combine functional properties—such as magnetic responsiveness—with biocompatibility. Moreover, the absence of cytotoxicity supports the feasibility of using such composites in applications ranging from tissue engineering scaffolds to magnetically

Journal of Materials Research and Technology 44 (2026) 3386–3397

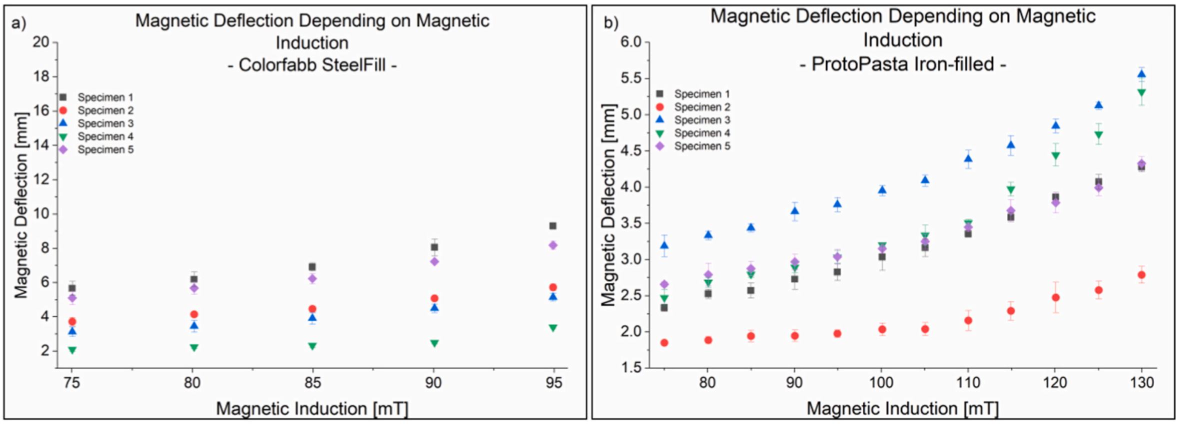

Fig. 10. Magnetic deflection depending on magnetic induction in the for CF SteelFill (a)) and PP Iron-filled (b)) materials.

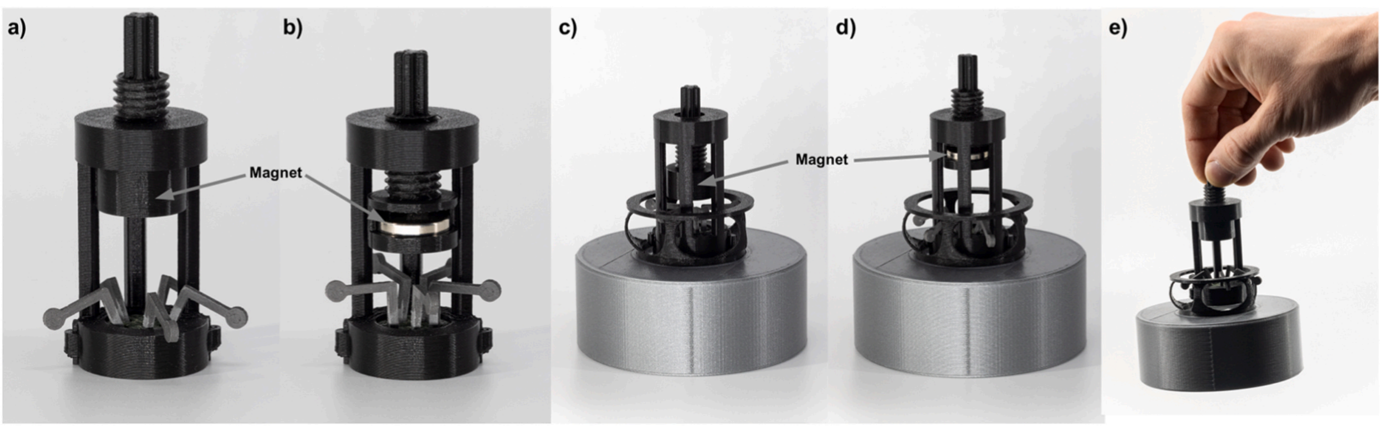

Fig. 11. *Demonstration of the operation of a magnetically controlled gripping mechanism.* ***a)*** *Default state of the structure.* ***b)-c)*** *By positioning the magnet closer to the magnetic composite, the structure transitions into a more compact state, facilitating its insertion into a hollow object.* ***d)-e)*** *The magnet is moved farther away from the magnetic composite, and the structure returns to its original state, catching on the object's rim from the inside and making the object liftable or movable.*

actuated devices.

However, within the context of a biomedical application, it is important to note that the study was limited to a 48-h incubation period. Therefore, further long-term research is required to ascertain whether these composites affect cell viability over an extended exposure period. This assertion is further substantiated by the observation that Iron-filled material underwent rust formation during extended periods of soaking in cell culturing medium.

A further limitation of this study is that only commercially available composites, containing stainless steel or iron powders, were investigated. Additionally, future work can extend the study by examining the properties of HTPLA (heat-treatable PLA) composites from the manufacturer ProtoPasta (High Density Stainless Steel-filled HTPLA and High Density Iron-filled HTPLA).

The present study provides insight into the mechanical and magnetic behavior of metal-filled polymer composites, which is particularly relevant given that the 3D printing of magnetic materials for medical applications is a relatively new and extensively researched topic [46]. The potential applications of these magnetic materials are manifold, they are being extensively investigated, particularly as scaffolds, in medicine and medical device research [47,48]. Magnetic scaffolds can be effective tools for tissue engineering and magnetic hyperthermia applications [47,49–51]. It is noteworthy that the majority of the scaffolds examined in the extant literature were not fabricated from off-the-shelf filaments. In future research, it will be valuable to examine the materials featured in the study that demonstrate a positive response to magnetic fields from this perspective. Another possible application for these materials is the fabrication of personalized magnetic orthoses and prostheses using 3D printing [52].

5. Conclusion

3D printing of magnetic materials has become a popular and timely research topic in recent years. Investigation of the mechanical, biological and magnetic properties of the commercially available magnetic filaments is necessary before using them for printing of medical devices. The present study investigated three magnetic PLA composites and compared them to pure PLA. Two of the composites examined are filled with stainless steel and one of them is filled with iron.

The materials under investigation did not demonstrate electrical conductivity, which would be beneficial. This phenomenon can be explained by the fact that the metal particles are not distributed homogeneously in the composite, and the amount of polymer is significantly greater than that of metal.

Two of the investigated materials (CF SteelFill and PP Iron-filled) have shown magnetic properties during the course of magnetic deflection tests.

None of the investigated materials has shown any cytotoxic effect, which indicates that these composites can be used for medical devices with skin contact for short-term. This enables the investigation of the usability of the 3D-printed parts from these polymer composites as a part of individualised orthoses or prostheses.

In light of the findings from the mechanical, structural, biological, and magnetic tests performed in the present study, the investigated

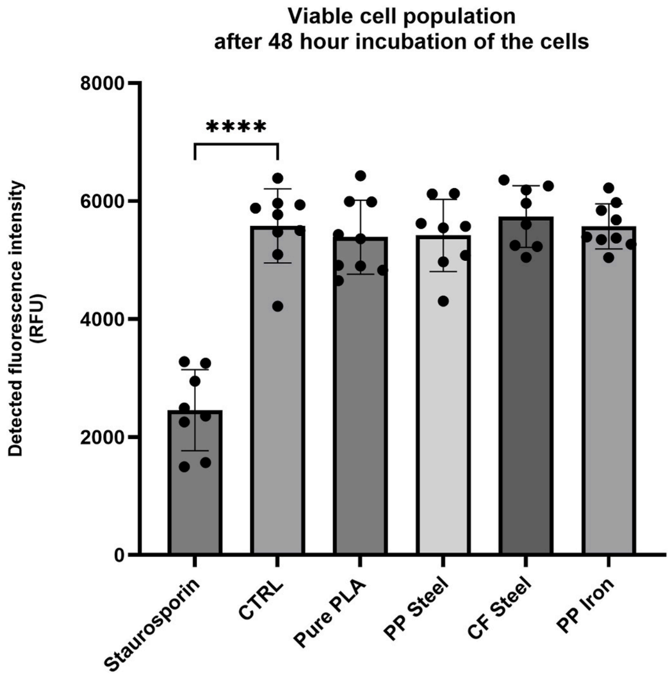

Fig. 12. Quantification of the living cell number after 48h incubation of A549 cells in the presence of 3D-printed non-magnetic inserts. Significant levels were labeled as follows: $p < 0.0332$ (*), $p < 0.0021$ (**), $p < 0.0002$ (***), and $p < 0.0001$ (****). Staurosporine is the positive control (cell death-inducing control); CTRL is the negative control. Abbreviations: PP: Protopasta, CF: ColorFabb.

materials have the potential to be used as materials for future 4D printing applications, particularly for orthotic and prosthetic devices.

Data statement

Kardos, Kinga; Paari-Molnar, Emese; Told, Roland; Qadan, Wa'el Nafith Abdel-Fattah; Szabó, Péter; Steinerbrunner-Nagy, Alexandra; Schlegl, Adam T.; Pongracz, Judit; Maroti, Peter (2026), “Dataset of Comprehensive Study of Mechanical, Structural, Magnetic and Biological Properties of Magnetic PLA Composites for 3D and 4D Printing Applications ”, Mendeley Data, V1, doi: 10.17632/prmn24vt6h.1In case of citing the data can be found in the “Supplementary Materials”, please, refer to the original article as well.

Author contributions

K.K.: Conceptualization, Data Curation, Formal analysis, Investigation, Methodology, Software, Validation, Visualization, Writing – original draft, E. P-M.: Conceptualization, Data Curation, Formal analysis, Investigation, Methodology, Software, Validation, Visualization, Writing – original draft, R.T.: Conceptualization, Data Curation, Formal analysis, Investigation, Methodology, Software, Validation, Writing – original draft, W.N.A-F.Q.: Investigation, Writing – original draft, P. Sz.: Visualization, Software, Methodology, A.S-N.: Methodology, Investigation, Data Curation, Validation, Writing – original draft, A.T.S.: Supervision, Validation, Writing – review and editing, J.E.P.: Project administration, Resources, Supervision, Validation, Wrinting – review and editing, P.M.: Conceptualization, Project administration, Founding acquisition, Resources, Supervision, Validation, Wrinting – review and editing.

Declaration of generative AI and AI-assisted technologies in the manuscript preparation process

During the preparation of this work the authors used Deepl SE in order to spell check. After using this tool/service, the authors reviewed and edited the content as needed and take full responsibility for the content of the published article.

Funding

The work was supported by the János Bolyai Research Scholarship of the Hungarian Academy of Sciences (BO/00213/23).

Declaration of competing interests

The authors declare that they have no known competing financial interests or personal relationships that could have appeared to influence the work reported in this paper.

Acknowledgement

We are thankful for the colleagues in the 3D printing and Visualization Centre for supporting this work. This work was supported by PTE ÁOK-KA No: 2023/2092.

Appendix A. Supplementary data

Supplementary data to this article can be found online at https://doi.org/10.1016/j.jmrt.2026.07.320.

References

[1] Kumar J, Mishra V, Negi S. An overview of research on FFF based additive manufacturing of polymer composite. In: Lecture notes in mechanical engineering; 2024. https://doi.org/10.1007/978-981-97-0900-7_17.

[2] Ahmadifar M, Benfriha K, Shirinbayan M, Tcharkhtchi A. Additive manufacturing of polymer-based composites using fused filament fabrication (FFF): a review. Appl Compos Mater 2021. https://doi.org/10.1007/s10443-021-09933-8.

[3] Mateti T, Jain S, Ananda Shruthi L, Laha A, Thakur G. An overview of the advances in the 3D printing technology. 3D Printing Technology for Water Treatment Applications 2023 Jan 1:1–37. https://doi.org/10.1016/B978-0-323-99861-1.00002-3.

[4] Mobarak MH, Abid AS, Munna MS, Dutta M, Rimon MIH. Additive manufacturing in biomedical: applications, challenges, and prospects. Hybrid Adv 2025. https://doi.org/10.1016/j.hybadv.2025.100467.

[5] Kumar P, Rajak DK, Abubakar M, Ali SGM, Hussain M. 3D printing technology for biomedical practice: a review. J Mater Eng Perform 2021 Jul 1;30(7):5342–55. https://doi.org/10.1007/S11665-021-05792-3/TABLES/2.

[6] Amin R, Hossaeini Marashi SM, Reza Noori SM, Alavi Z, Dehghani E, Maleki R, et al. Medical, pharmaceutical, and nutritional applications of 3D-printing technology in diabetes. Diabetes Metabol Syndr: Clin Res Rev 2024 Apr 1;18(4):103002. https://doi.org/10.1016/J.DSX.2024.103002. PubMed PMID: 38615569.

[7] Told R, Kardos K, Paari-Molnar E, Szabo G, Ujfalusi Z, Sahai N, et al. Comparative analysis of mechanical and thermal characteristics of 3D-Printed polyamide using material extrusion and powder bed fusion process with industrial and desktop printers. Macromol Mater Eng 2025 Feb 1;310(2):2400293. https://doi.org/10.1002/MAME.202400293.

[8] Kardos K, Told R, Pentek A, Sahai N, Banfai K, Vizi A, et al. Surface disinfection change the mechanical, structural and biological properties of flexible materials used for additive manufacturing of medical devices. Mater Des 2024 Jan 1;237:112616. https://doi.org/10.1016/J.MATDES.2023.112616.

[9] Paari-Molnar E, Kardos K, Told R, Simon I, Sahai N, Szabo P, et al. Comprehensive study of mechanical, electrical and biological properties of conductive polymer composites for medical applications through additive manufacturing. Polymers 2024;16:2625. https://doi.org/10.3390/POLYM16182625. 2024 Sep 17;16(18):2625.

[10] Rendeki S, Nagy B, Bene M, Pentek A, Toth L, Szanto Z, et al. An overview on Personal Protective Equipment (PPE) fabricated with additive manufacturing technologies in the era of COVID-19 pandemic. Polymers 2020 Nov 16;12(11):1–18. https://doi.org/10.3390/POLYM12112703. 2020, Vol 12.

[11] Hasanzadeh R, Jolaiy S, Mojaver M, Azdast T, Park CB. Auxetic 3D printed metastructure stents for enhanced mechanical and structural performance and biocompatibility in coronary artery treatments. Acta Biomater 2025 Aug 1;202:641–59. https://doi.org/10.1016/J.ACTBIO.2025.06.043. PubMed PMID: 40581033.

[12] Hasanzadeh R. Polylactic acid/carbon fiber composites in 3D printing: analysis and multi-objective optimization of structural and mechanical performance using box–Behnken technique. Int J Struct Integr 2025:1–22. https://doi.org/10.1108/IJSI-03-2025-0062/1278919.
[13] Hasanzadeh R. Machine learning-driven optimization of energy absorption in PLA composites reinforced with carbon fibers through FFF additive manufacturing. Rapid Prototyp J 2025:1–11. https://doi.org/10.1108/RPJ-06-2025-0219/1311614.
[14] Hasanzadeh R, Mihankhah P, Azdast T, Bodaghi M, Moradi M. Process-property relationship in polylactic acid composites reinforced by iron microparticles and 3D printed by fused filament fabrication. Polym Eng Sci 2024 Jan 1;64(1):399–411. https://doi.org/10.1002/PEN.26556.
[15] Tedla G, Rogers K. Characterization of 3D printing filaments containing metal additives and their particulate emissions. Sci Total Environ 2023 Jun 1;875:162648. https://doi.org/10.1016/J.SCITOTENV.2023.162648. PubMed PMID: 36906034.
[16] Petousis M, Vidakis N, Mountakis N, Papadakis V, Kanellopoulou S, Gaganatsiou A, et al. Multifunctional material extrusion 3D-Printed antibacterial polylactic acid (PLA) with binary inclusions: the effect of cuprous oxide and cellulose nanofibers. Fibers 2022;10(6). https://doi.org/10.3390/FIB10060052. Vol 10,. 2022 Jun 10.
[17] Vidakis N, Petousis M, Velidakis E, Mountakis N, Tzounis L, Liebscher M, et al. Enhanced mechanical, thermal and antimicrobial properties of additively manufactured polylactic acid with optimized nano silica content. Nanomaterials 2021;11(4). https://doi.org/10.3390/NANO11041012. Vol 11,. 2021 Apr 15.
[18] Vidakis N, Moutsopoulou A, Petousis M, Michailidis N, Charou C, Mountakis N, et al. Medical-grade PLA nanocomposites with optimized tungsten carbide nanofiller content in MEX additive manufacturing: a rheological, morphological, and thermomechanical evaluation. Polymers 2023;15(19). https://doi.org/10.3390/POLYM15193883. 2023 Sep 25;15.
[19] Ranjan N, Kumar R, Kumar S, Kumar D, Saxena KK. Innovative high-performance metal reinforced polymers composites for 3D printing applications: a review. Advances in Materials and Processing Technologies 2024 Jul 2;10(3):1800–13. https://doi.org/10.1080/2374068X.2023.2202527.
[20] Buj-Corral I, Sanz-Fraile H, Ulldemolins A, Tejo-Otero A, Domínguez-Fernández A, Almendros I, et al. Characterization of 3D printed Metal-PLA composite scaffolds for biomedical applications. Polymers 2022;14:2754. https://doi.org/10.3390/POLYM14132754. 2022 Jul 5;14(13):2754.
[21] Kardos K, Paari-Molnar E, Told R, Len A, Szabo P, Ujfalusi Z, et al. Characterization of Copper- and bronze-filled PLA: mechanical, structural, and biological insights for biomedical 3D and 4D printing. Macromol Mater Eng 2025 Oct;11:e00316. https://doi.org/10.1002/MAME.202500316.
[22] Tibbits S. 4D printing: multi-material shape change. Archit Des 2014 Jan 1;84(1):116–21. https://doi.org/10.1002/AD.1710.
[23] Mazeeva A, Masaylo D, Razumov N, Konov G, Popovich A. 3D printing technologies for fabrication of magnetic materials based on metal–polymer composites: a review. Materials 2023 Oct 28;16(21):6928. https://doi.org/10.3390/MA16216928. 2023, Vol 16, Page 6928.
[24] Martinez L, Palessonga D, Roquefort P, Chevalier A, Maalouf A, Ville J, et al. Development of a high temperature printable composite for microwave absorption applications. AIMS Mater Sci 2021;8(5):739–47. https://doi.org/10.3934/MATERSCI.2021044.
[25] Amirov A, Omelyanchik A, Murzin D, Kolesnikova V, Vorontsov S, Musov I, et al. 3D printing of PLA/magnetic ferrite composites: effect of filler particles on magnetic properties of filament. Processes 2022 Nov 16;10(11):2412. https://doi.org/10.3390/PR10112412. 2022, Vol 10, Page 2412.
[26] Lalegani Dezaki M, Bodaghi M. Sustainable 4D printing of magneto-electroactive shape memory polymer composites. Int J Adv Manuf Technol 2023 May 1;126(1–2):35–48. https://doi.org/10.1007/S00170-023-11101-0/FIGURES/8.
[27] Bernier F, Ibrahim M, Mihai M, Thomas Y, Lamarre JM. Additive manufacturing of soft and hard magnetic materials used in electrical machines, vol. 75; 2021 Nov 8. p. 334–43. https://doi.org/10.1016/J.MPRP.2019.12.002. 6.
[28] Guan XN, Xu XN, Kuniyoshi R, Zhou HH, Zhu YF. Electromagnetic and mechanical properties of carbonyl iron powders-PLA composites fabricated by fused deposition modeling. Mater Res Express 2018 Sep 12;5(11):115303. https://doi.org/10.1088/2053-1591/AADCE4.
[29] Díaz-García Á, Law JY, Felix M, Guerrero A, Franco V. Functional, thermal and rheological properties of polymer-based magnetic composite filaments for additive manufacturing. Mater Des 2022 Jul 1;219:110806. https://doi.org/10.1016/J.MATDES.2022.110806.
[30] Cao X, Xuan S, Sun S, Xu Z, Li J, Gong X. 3D printing magnetic actuators for biomimetic applications. ACS Appl Mater Interfaces 2021 Jun 30;13(25):30127–36. https://doi.org/10.1021/ACSAMI.1C08252/SUPPL_FILE/AM1C08252_SI_003. MP4 PubMed PMID: 34137263.
[31] Zhao W, Huang Z, Liu L, Wang W, Leng J, Liu Y. Porous bone tissue scaffold concept based on shape memory PLA/Fe3O4. Compos Sci Technol 2021 Feb 8;203:108563. https://doi.org/10.1016/J.COMPSCITECH.2020.108563.
[32] Guessasma S, Belhabib S. Effect of the printing angle on the microstructure and tensile performance of iron-reinforced polylactic acid composite manufactured using fused filament fabrication. J Manuf Mater Process 2024 Mar 27;8(2):65. https://doi.org/10.3390/JMMP8020065. 2024, Vol 8, Page 65.
[33] Pan D, Al Mamun A, Zhou R, Bappy MM, Islam MS. Comprehensive and comparative characterizations of tensile properties and fracture mechanisms of 3D printed multifunctional carbon-fiber and metal-filled PLA composite parts. Polym Compos 2025;0:1–19. https://doi.org/10.1002/PC.70281.
[34] Alnajjar BMK, Buchau A, Baumgärtner L, Anders J. NMR magnets for portable applications using 3D printed materials. J Magn Reson 2021 May 1;326:106934. https://doi.org/10.1016/J.JMR.2021.106934. PubMed PMID: 33684681.
[35] Nyilvános megosztás - Fájlok - colorFabb [Internet]. [cited 2026 Jul 20]. Available from: https://downloads.colorfabb.com/index.php/s/rtfDDRCa723Xdor?path=/.
[36] Material data table – protoplant, makers of protopasta [Internet]. [cited 2026 Jul 20]. Available from: https://proto-pasta.com/pages/material-data-table.
[37] ISO 291:2008 - Plastics — standard atmospheres for conditioning and testing [Internet]. [cited 2026 Jul 20]. Available from: https://www.iso.org/standard/50572.html.
[38] International Organization for Standardization. ISO 527-1:2019 plastics determination of tensile properties part 1: general principles. Ics 8308001 [Internet]. 2019 [cited 2025 Oct 10]. Available from: https://www.iso.org/standard/75824.html.
[39] International Organization for Standardization. ISO 178:2019 plastics determination of flexural properties. International Standard; 2019 [Internet] [cited 2025 Oct 10]. Available from: https://www.iso.org/standard/70513.html.
[40] International Organization for Standardization. ISO 179-1:2010 plastics — determination of charpy impact properties — part 1: non-Instrumented impact test [Internet] [cited 2025 Oct 10]. Available from: https://www.iso.org/standard/44852.html; 2010.
[41] International Organization for Standardization. ISO 868:2003 plastics and ebonite — determination of indentation hardness by means of a durometer (shore hardness) [Internet] [cited 2025 Oct 10]. Available from: https://www.iso.org/standard/34804.html; 2003.
[42] Kelava L, Ivić I, Pakai E, Fekete K, Maroti P, Told R, et al. Stereolithography 3D printing of a heat exchanger for advanced temperature control in wire myography. Polymers 2022;14:471. https://doi.org/10.3390/POLYM14030471. 2022 Jan 25;14(3):471.
[43] Nicolas roduit. JMicroVision.
[44] Vakharia VS, Kuentz L, Salem A, Halbig MC, Salem JA, Singh M. Additive manufacturing and characterization of metal particulate reinforced polylactic acid (PLA) polymer composites. Polymers 2021 Oct 14;13(20):3545. https://doi.org/10.3390/POLYM13203545. 2021, Vol 13, Page 3545.
[45] Laureto J, Tomasi J, King JA, Pearce JM. Thermal properties of 3-D printed polylactic acid-metal composites. Progr Addit Manuf 2017 Jun 1;2(1–2):57–71. https://doi.org/10.1007/S40964-017-0019-X/FIGURES/15.
[46] Rezaei B, Moni HEJ, Karampelas IH, Sharma A, Mostufa S, Azizi E, et al. Additive manufacturing of magnetic materials for energy, environment, healthcare, and industry applications. Adv Funct Mater 2025 Mar 4;35(10):2416823. https://doi.org/10.1002/ADFM.202416823;ISSUE:ISSUE.
[47] Fernandes PD, Silva FC, Magalhães FD, Pereira RF, Santos SG, Pinto AM. 3D printing of nanoparticle-containing scaffolds for cancer phototherapy, magnetic hyperthermia therapy, and tissue regeneration. Acta Biomater 2025 Nov;25. https://doi.org/10.1016/J.ACTBIO.2025.11.043.
[48] Marovič N, Ban I, Maver U, Maver T. Magnetic nanoparticles in 3D-printed scaffolds for biomedical applications. Nanotechnol Rev 2023 Jan 1;12(1). https://doi.org/10.1515/NTREV-2022-0570/XML.
[49] Alexandridis A, Argyros A, Kyriazopoulos P, Genitseftsis I, Okkalidis N, Michailidis N, et al. Composite magnetic filaments: from fabrication to magnetic hyperthermia application. Micromachines 2025 Mar 1;16(3):328. https://doi.org/10.3390/MI16030328/S1.
[50] Alam F, Varadarajan KM, Kumar S. 3D printed polylactic acid nanocomposite scaffolds for tissue engineering applications. Polym Test 2020 Jan 1;81:106203. https://doi.org/10.1016/J.POLYMERTESTING.2019.106203.
[51] Yun HM, Ahn SJ, Park KR, Kim MJ, Kim JJ, Jin GZ, et al. Magnetic nanocomposite scaffolds combined with static magnetic field in the stimulation of osteoblastic differentiation and bone formation. Biomaterials 2016 Apr 1;85:88–98. https://doi.org/10.1016/J.BIOMATERIALS.2016.01.035. PubMed PMID: 26854394.
[52] Coburn KA, DeGrasse NS, Allyn KJ, Larsen BG, Garbini JL, Sanders JE. Using magnetic panels to enlarge a transtibial prosthetic socket. Med Eng Phys 2022 Dec 1;110:103924. https://doi.org/10.1016/J.MEDENGPHY.2022.103924. PubMed PMID: 36564131.